



CONSORZIO RFX
Ricerca Formazione Innovazione



EUROfusion



FIRST MEASUREMENTS OF BEAM PLASMA IN NIFS TEST STAND

E. Sartori^{1,3}, H. Nakano², P. Veltri^{1,4}, M. Kasaki², A. Pimazzoni¹, M. Brombin¹, V. Antoni¹, K. Ikeda², K. Tsumori² and G. Serianni¹

¹Consorzio RFX, Corso Stati Uniti 4 – 35127, Padova (Italy)

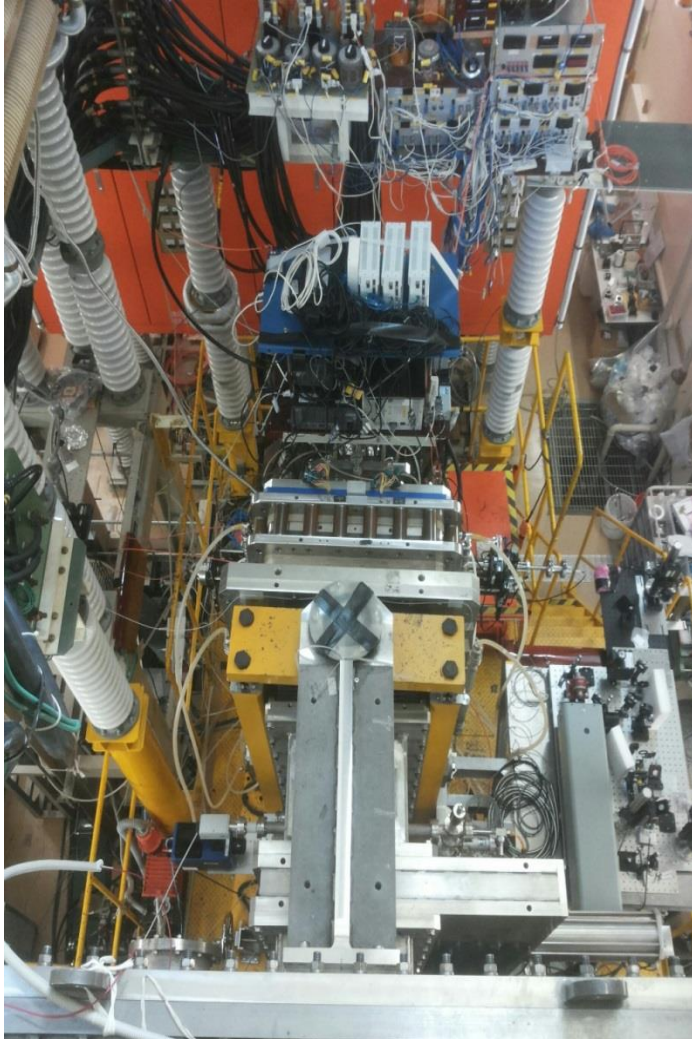
²National Institute for Fusion Science, 322-6 Oroshi, Toki, Gifu 509-5292, Japan

³University of Padova, Dept. of Management and Engineering, Strad. S. Nicola 3, 36100 Vicenza, Italy

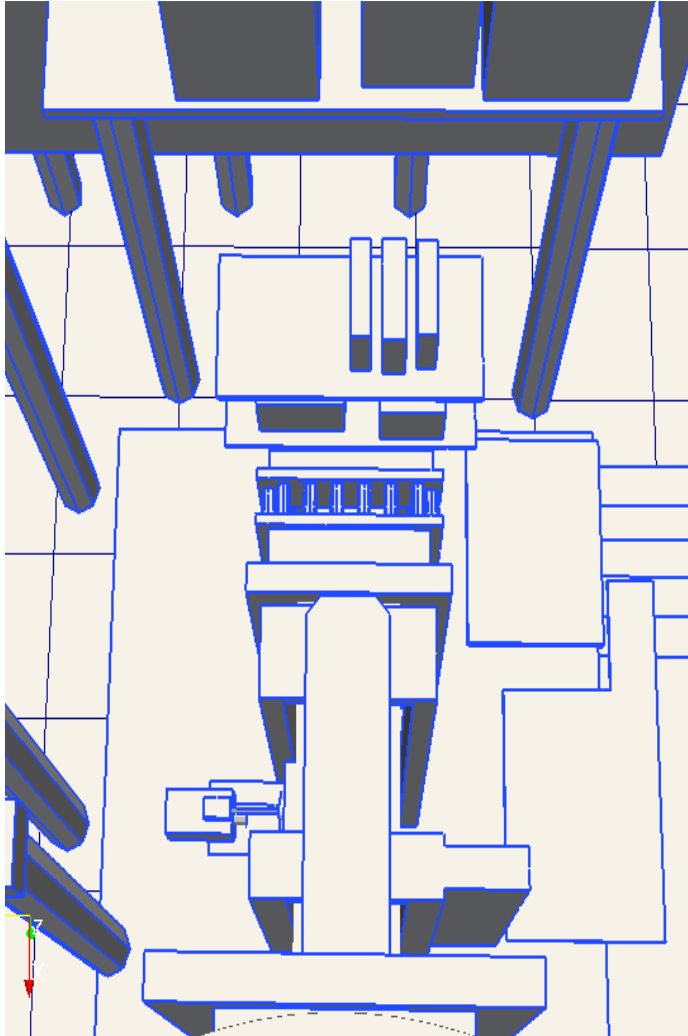
⁴INFN-LNL, Viale dell'Università 2, I-35020, Legnaro (Italy)



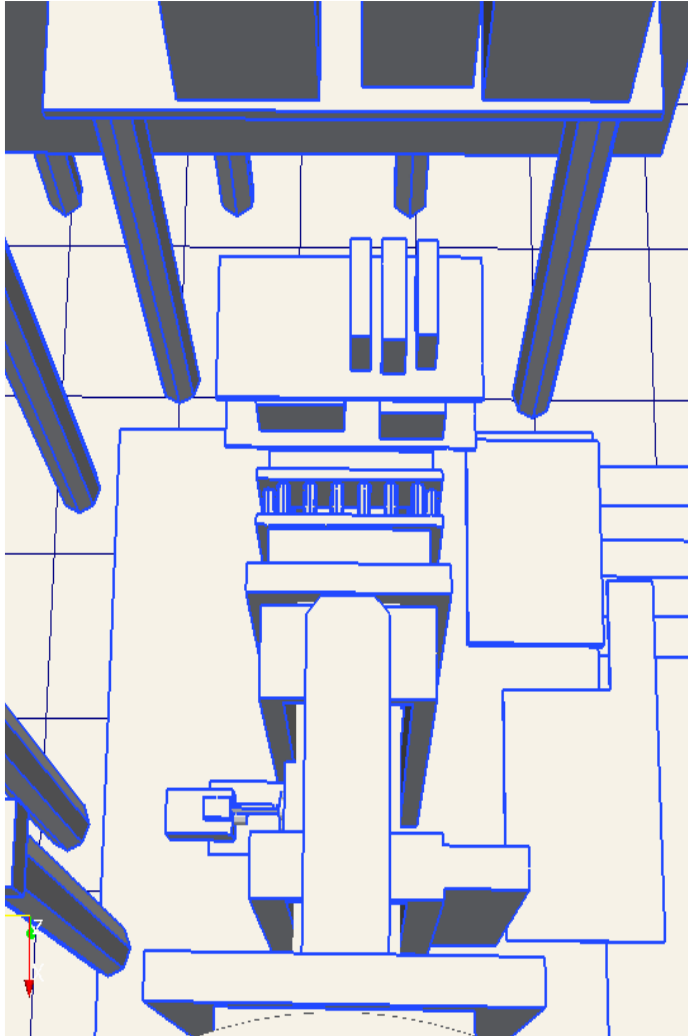
- Beam-generated plasma important for
 - Space Charge Compensation (propagation, optics & focusing)
 - positive ions backstreaming in the accelerator (heat load)
 - neutralization (efficiency)
 - Ion beam transport at low pressures (photoneutralizer?)
- **Effect of background gas pressure**
- **Multibeamlet H^- beam for Neutral Beams**
- Experimental study in multibeamlet negative ion beams: *R&D Negative Ion Source* in NIFS, Japan
 - Retarding Field Energy Analyser was designed and built to the purpose
- PIC Numerical simulations to support the experimental campaign



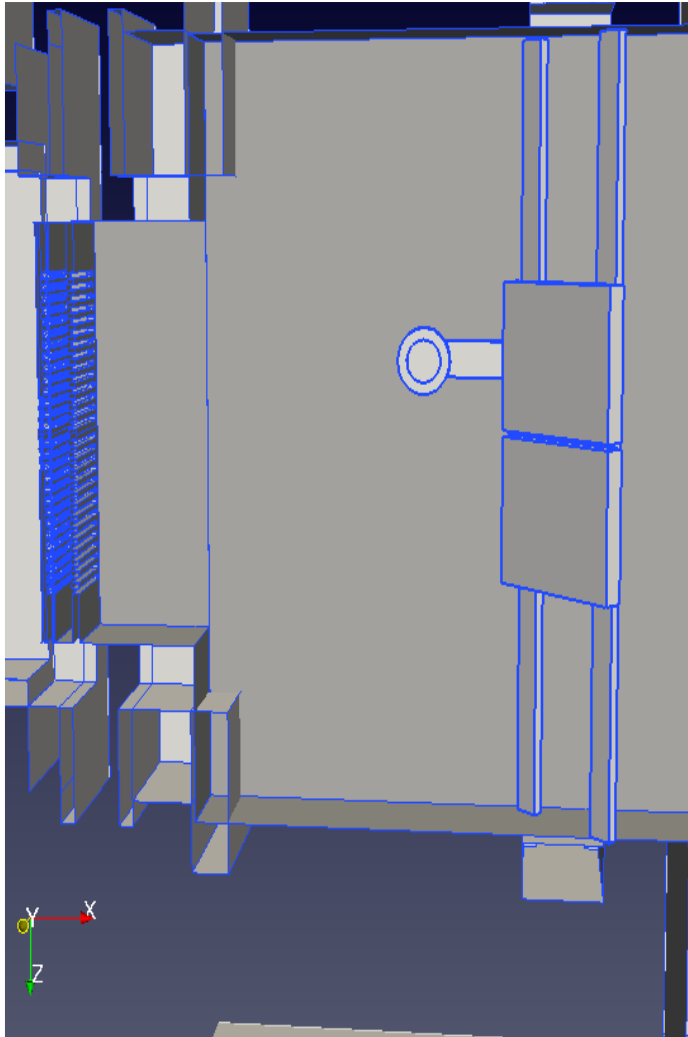
- H- beam
- Cesium surface-plasma negative ion source
- Hundreds of independent beamlets
- Beam energy for this campaign: $\sim 48\text{kV}$

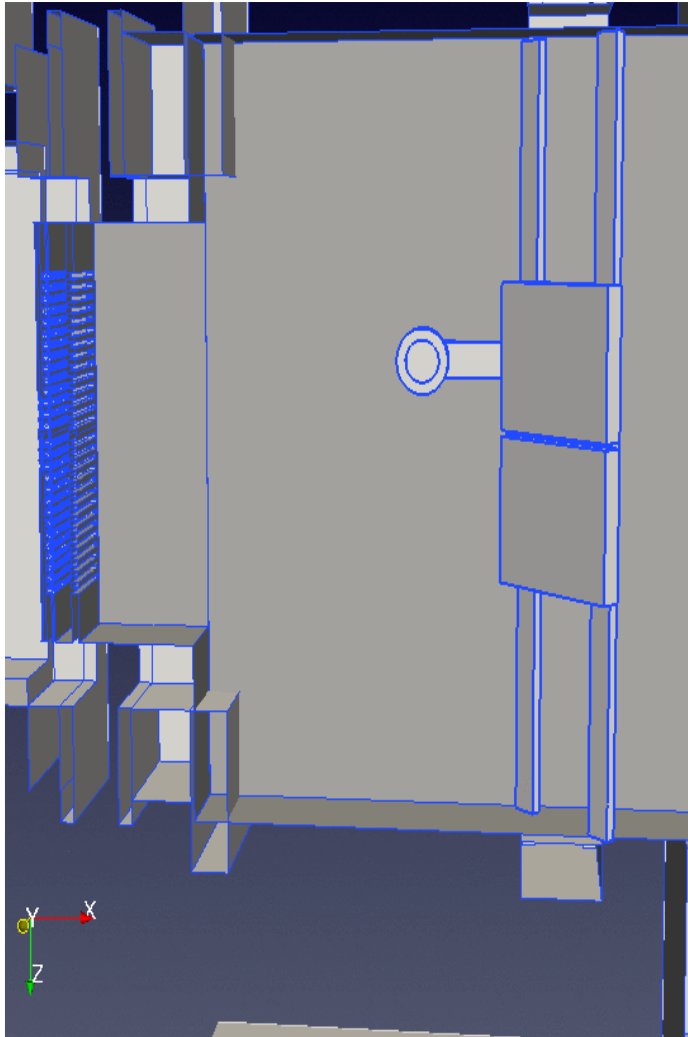


- H- beam
- Cesium surface-plasma negative ion source
- Hundreds of independent beamlets
- Beam energy for this campaign: $\sim 48\text{kV}$



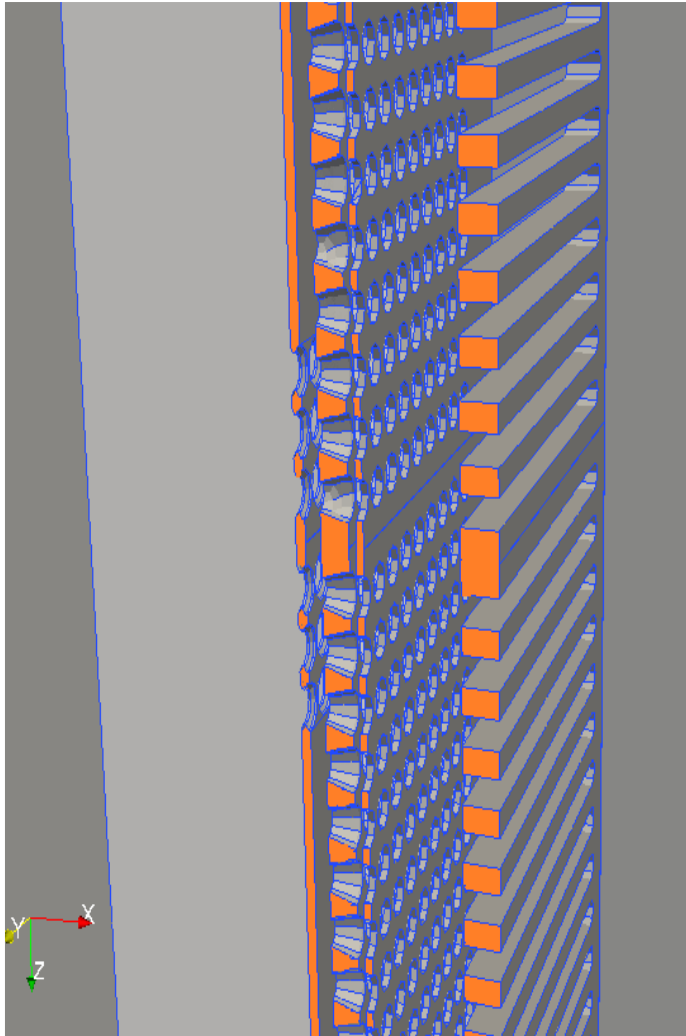
- H- beam
- Cesium surface-plasma negative ion source
- Hundreds of independent beamlets
- Beam energy for this campaign: $\sim 48\text{kV}$





Four multiaperture electrodes:

- Plasma Grid (PG)
- Extraction Grid (EXG)
Steering Grid (ESG)
- Grounded Grid (GG)

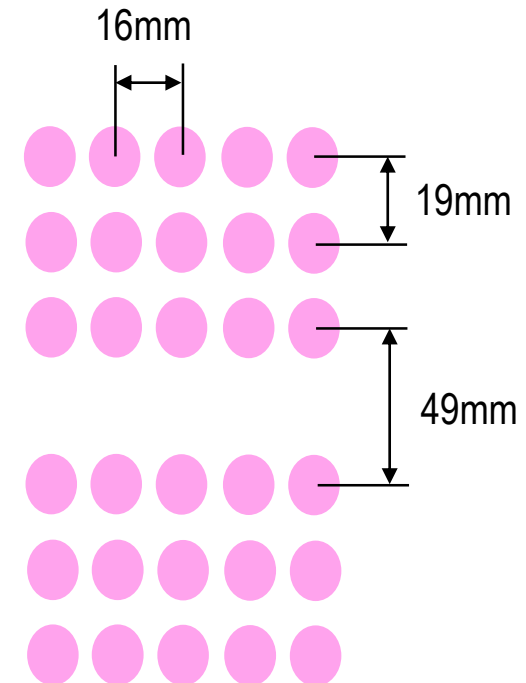


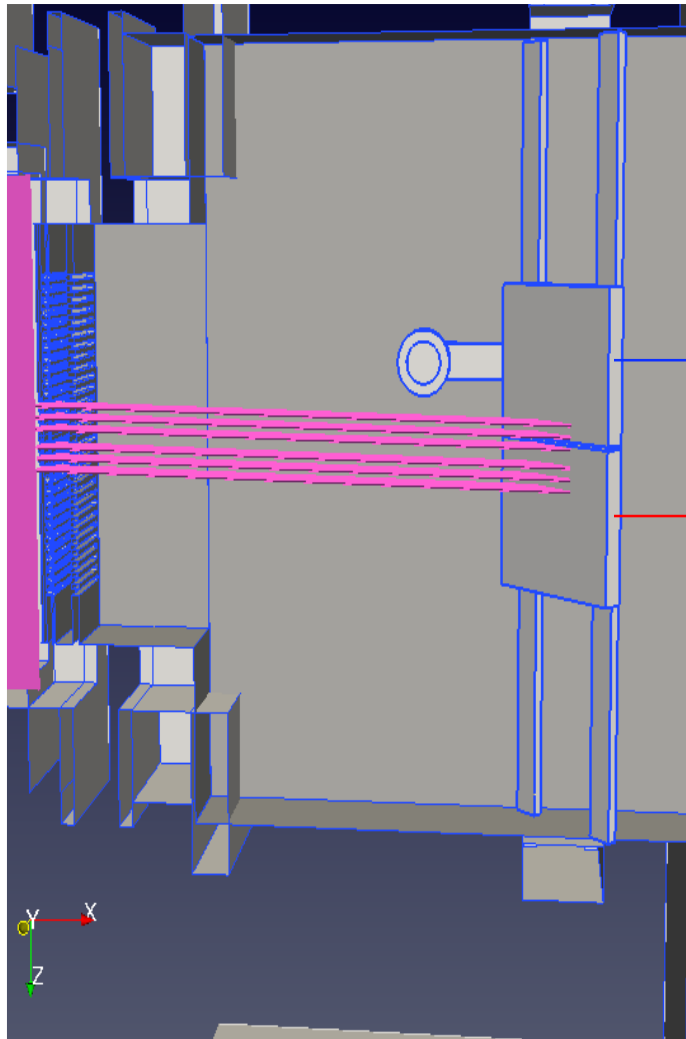
Four multiaperture electrodes:

- Plasma Grid (PG)
- Extraction Grid (EXG)
Steering Grid (ESG)
- Grounded Grid (GG)

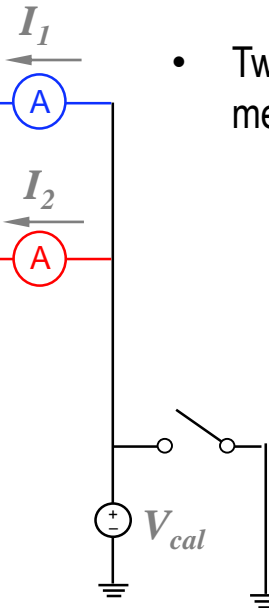
PG mask: reduced number of apertures:

- 30 beamlets
- Two 5x3 beamlet groups

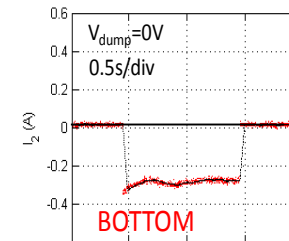
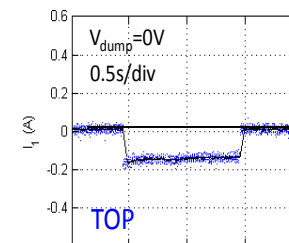




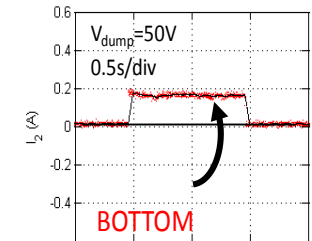
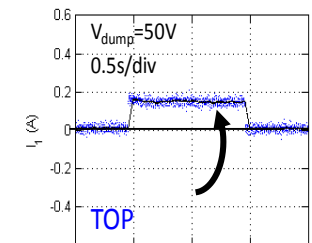
- graphite tiles, 45° to beam axis
- Insulated,
- Secondary electron emission: can be biased V_{cal}
- Two independent current measurements I_1, I_2

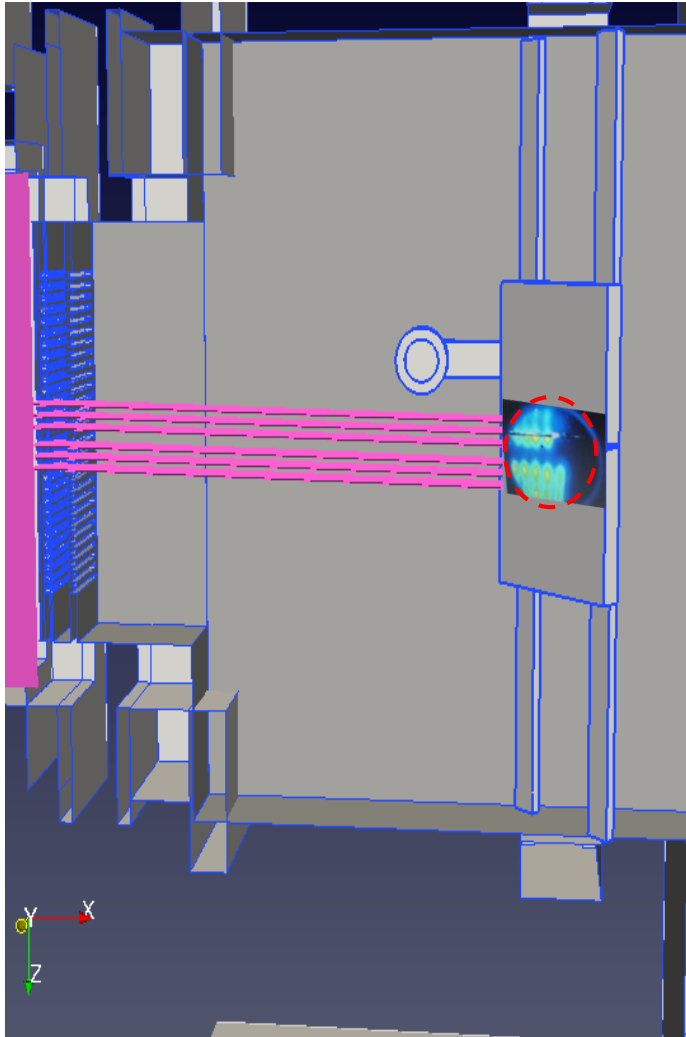


$V_{cal} = 0V$

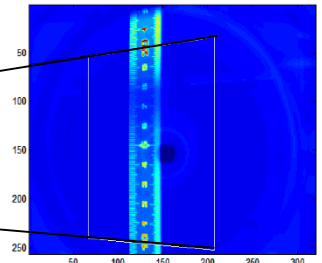
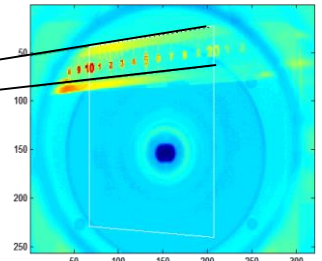


$V_{cal} = 50V$

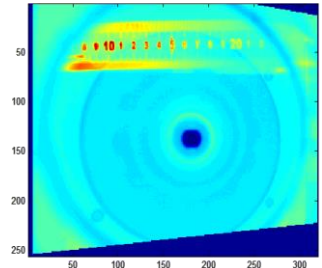


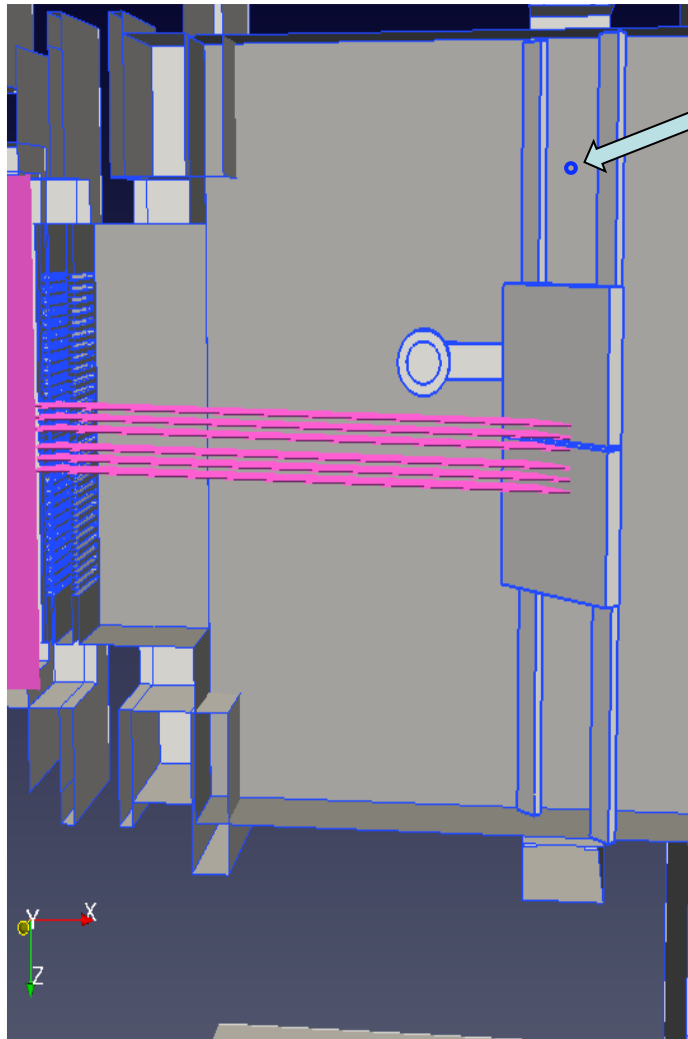


- Correction of perspective



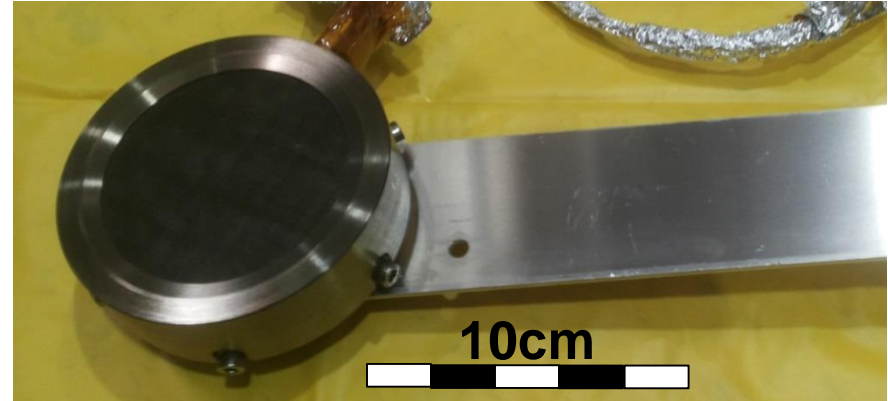
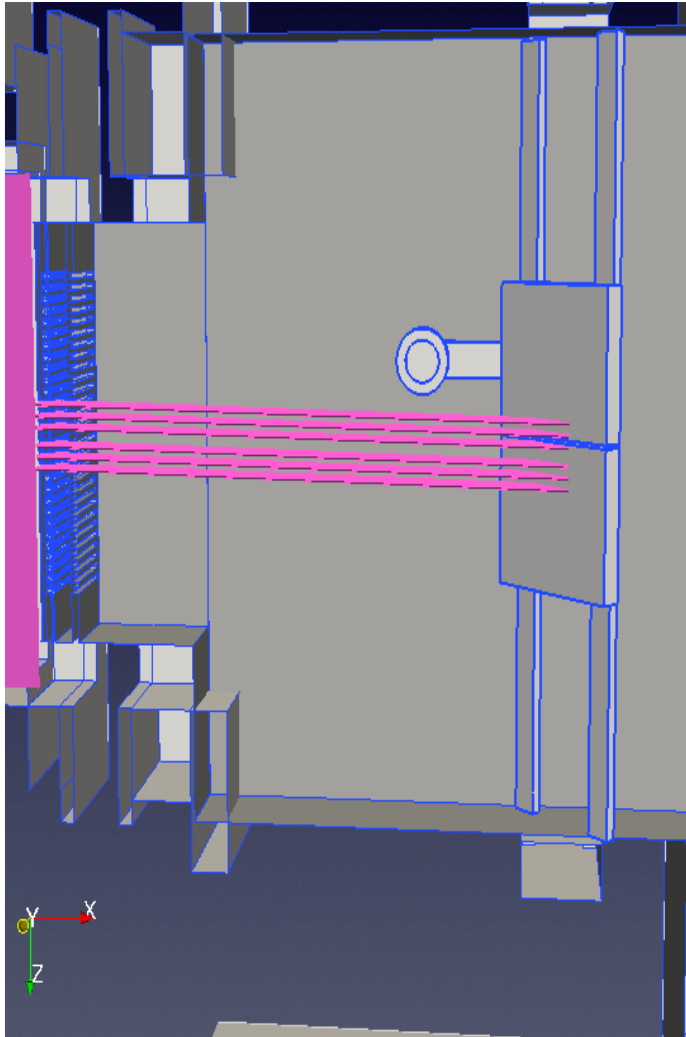
- Calibration of IR image resolution:
~2 pixel/mm
(along transverse direction x)



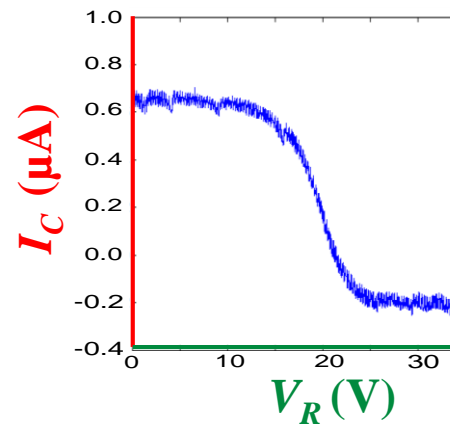


- Gas injection nozzle
- Control the gas density in drift region separately from the ion source

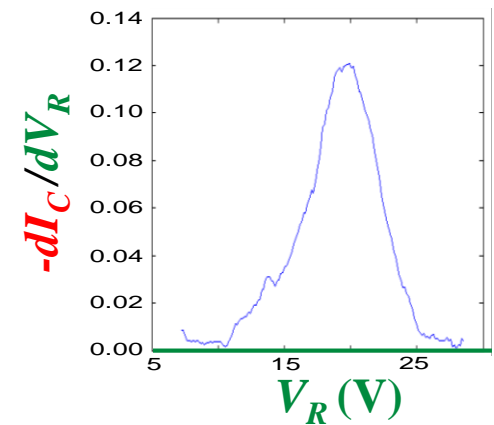
$$1.8 \text{ mPa} < p < 30 \text{ mPa}$$



Discriminates ions according to their energy.
Measures the integral ion parallel energy distribution:

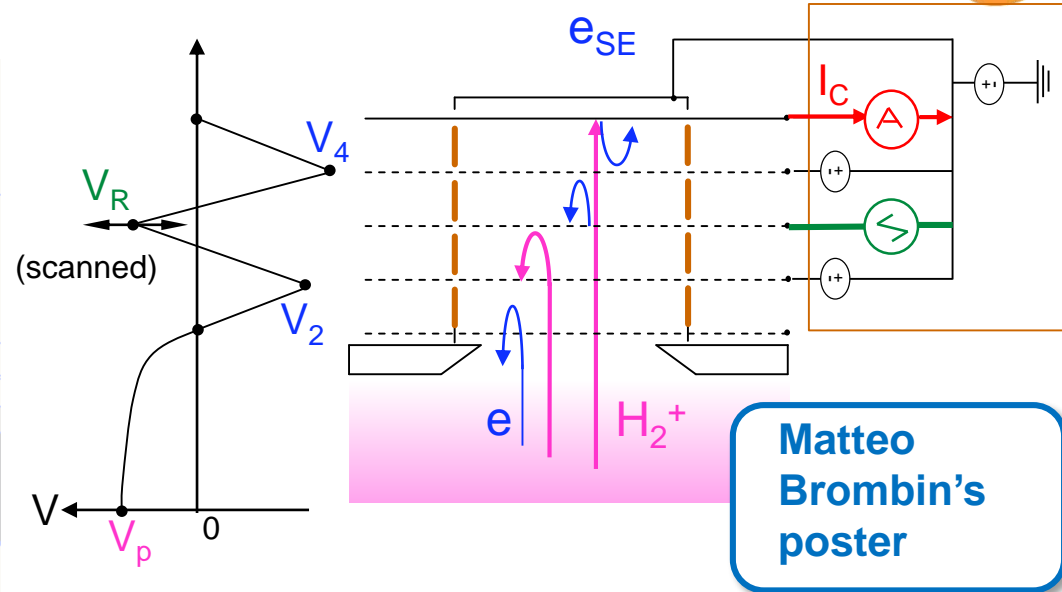
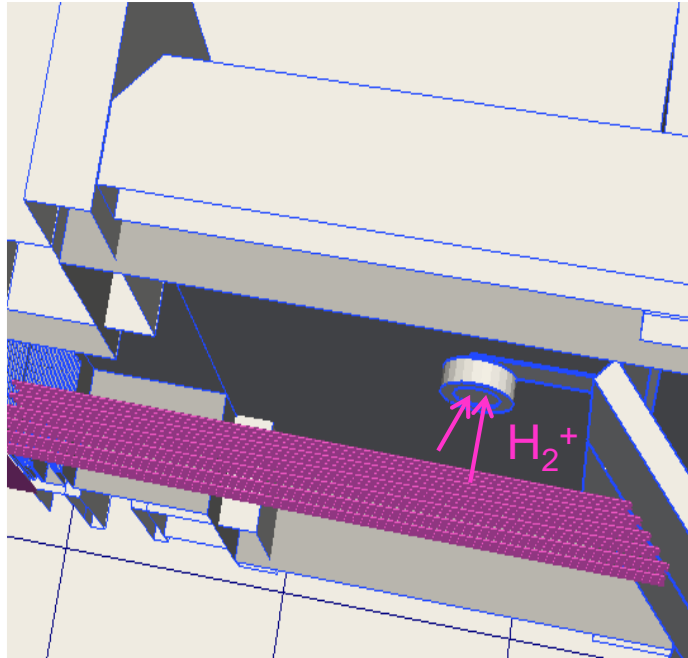


Current-voltage
characteristic



numerical differentiation
of the characteristic

4-GRIDS RETARDING FIELD ENERGY ANALYSER



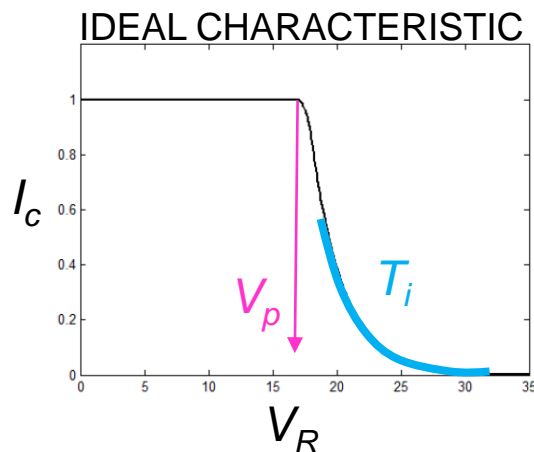
Collects positive ions exiting from the compensation plasma: integral parallel velocity distribution

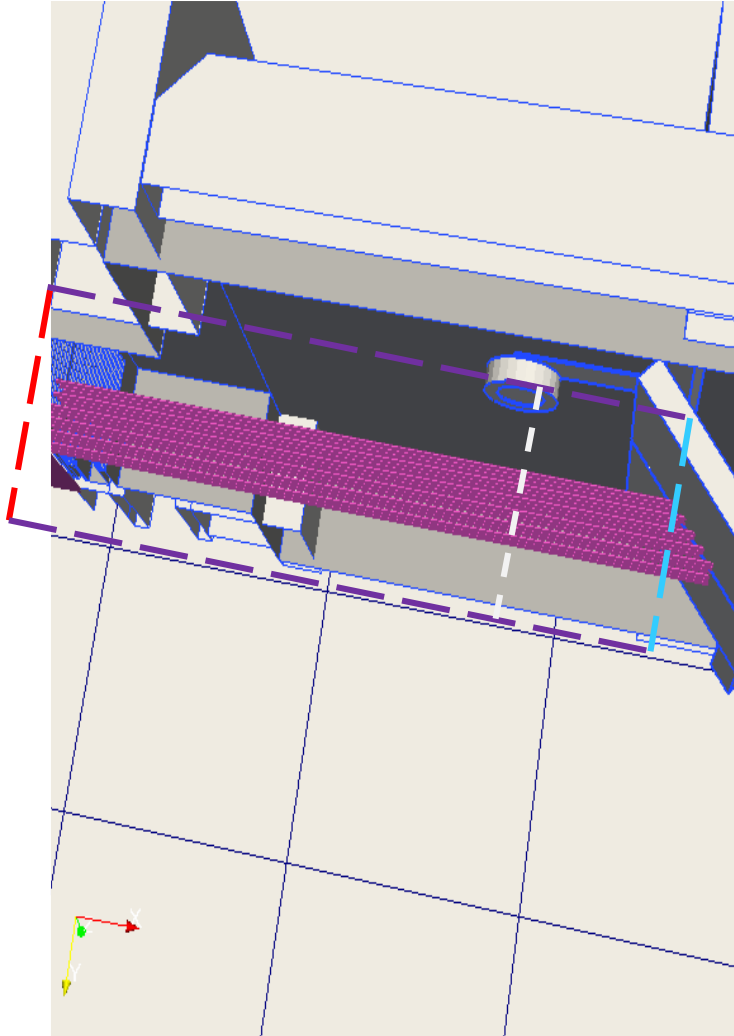
$$j_c = j_0 q_i K \int_u^\infty v_{||} f(v_{||}) dv_{||}$$

Non collisional sheath, Maxwellian plasma:

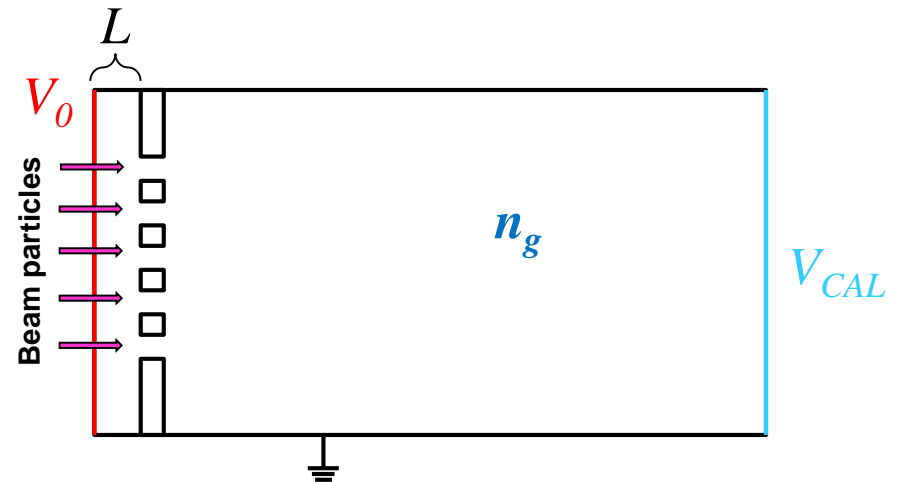
$$j_c = K \exp\left(-\frac{q_i(V_R - V_P)}{kT_i}\right), \text{ for } V_R > V_P$$

Complex transfer function may deform characteristics





- 2D 3V PIC-MCC code, GPGPU (CUDA)
- 6 species: e, H⁻, H, H⁺, H₂⁺, H₃⁺
26 processes
differential cross-sections
- Beam dump with bias (V_{cal}) and **secondary emission electrons**
- **Acceleration field:** $V_0 = -V_{acc} \frac{L}{L_{EXG-GG}}$



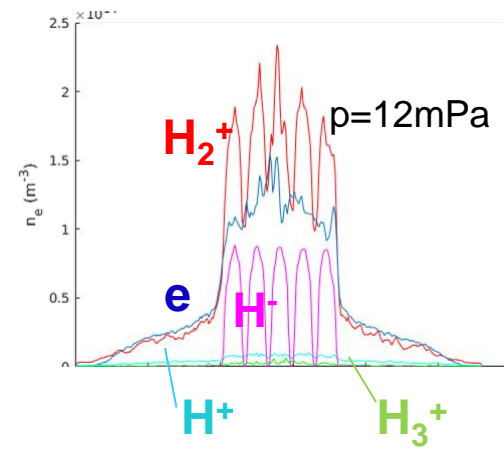
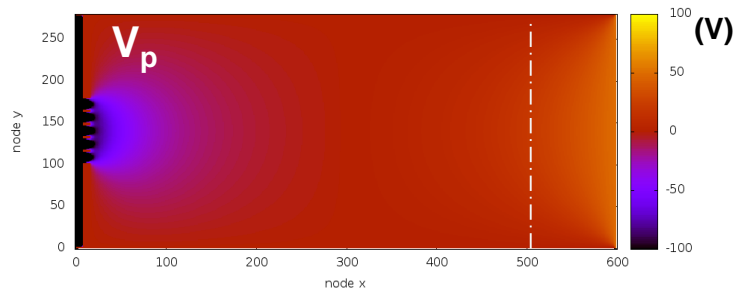
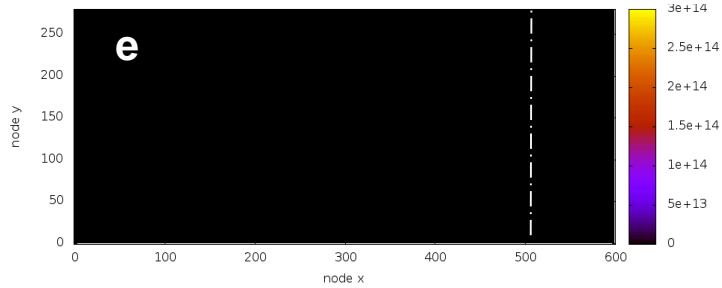
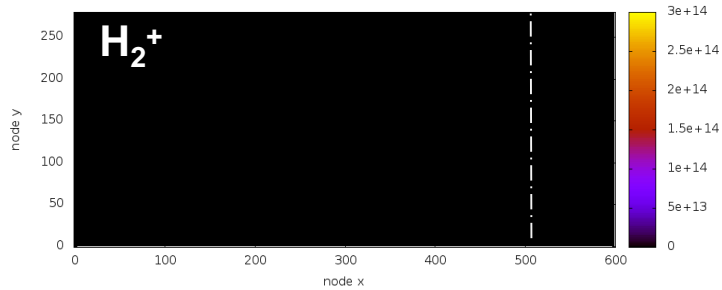
ADDITIONAL DIAGNOSTICS: NUMERICAL SIMULATION



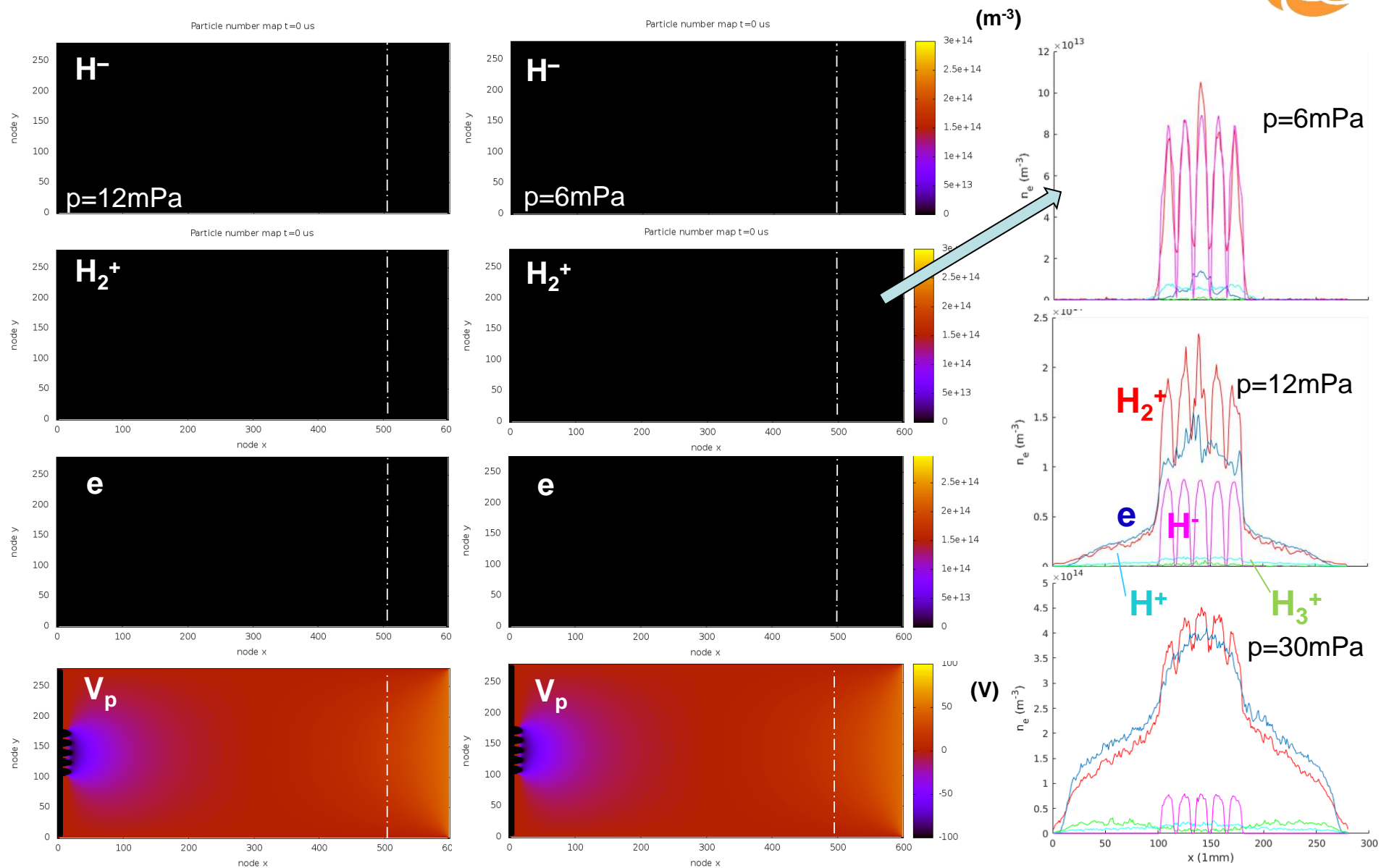
Particle number map t=0 us



Particle number map t=0 us



ADDITIONAL DIAGNOSTICS: NUMERICAL SIMULATION



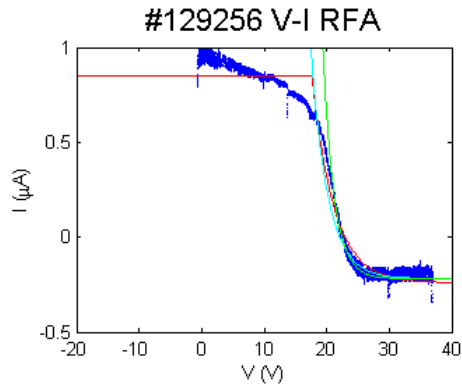
EXPERIMENTAL RESULTS:

- 1) Plasma potential
- 2) Temperatures
- 3) Effect on beam optics

1) RFA CHARACTERISTICS: PLASMA POTENTIAL

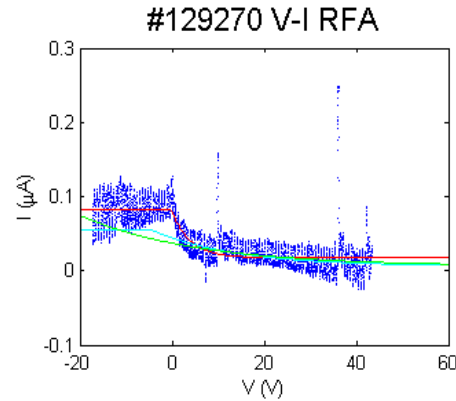


ION MODE

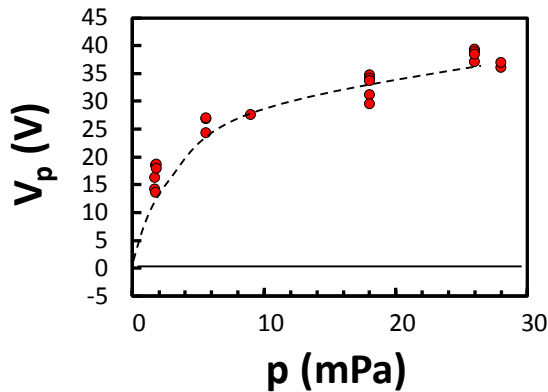


IEDF $V_b=50V$ $p=26mPa$

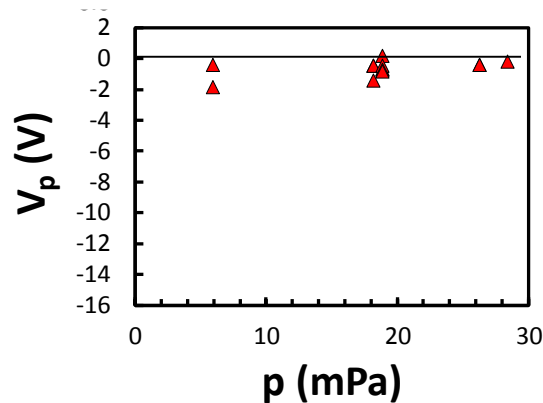
ELECTRON MODE



EEDF $V_b=50V$ $p=28.4mPa$



- ion mode, beam dump bias 0V
- ion mode, beam dump bias 50V



- ▲ electron mode, beam dump bias 0 V
- ▲ electron mode, beam dump bias 50 V

●, ▲ calorim. 50V
 Plasma potential from
 ion mode: $0 < V_p < V_{cal}$

1) RFA CHARACTERISTICS: PLASMA POTENTIAL

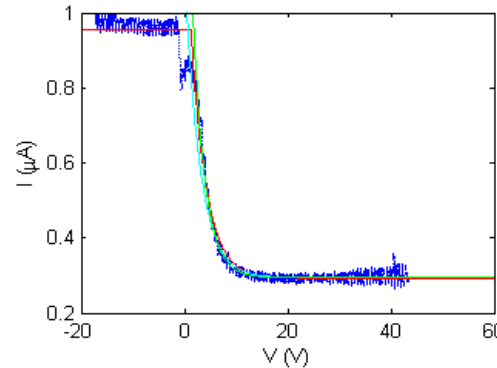
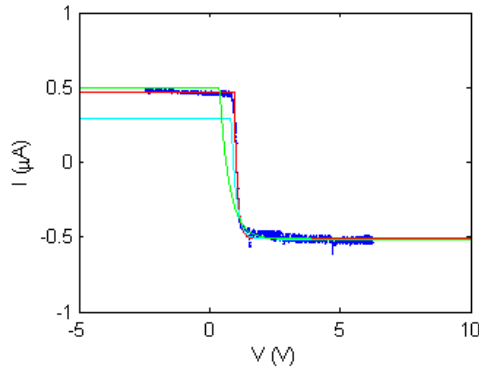


ION MODE

ELECTRON MODE

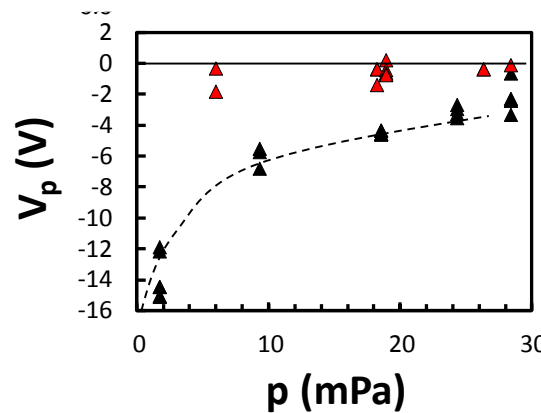
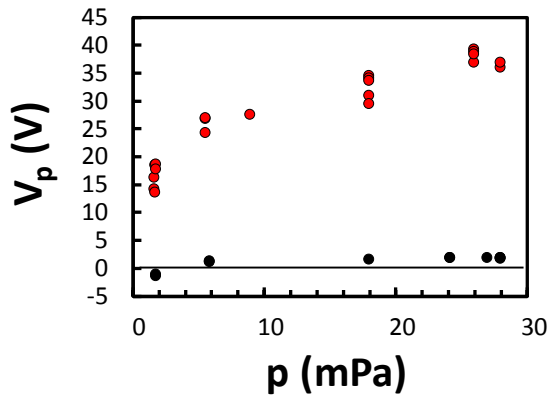
#129282 V-I RFA

#129271 V-I RFA



IEDF $V_b=0V$ $p=28mPa$

EEDF $V_b=0V$ $p=28.4mPa$



- ion mode, beam dump bias 0V
- ion mode, beam dump bias 50V

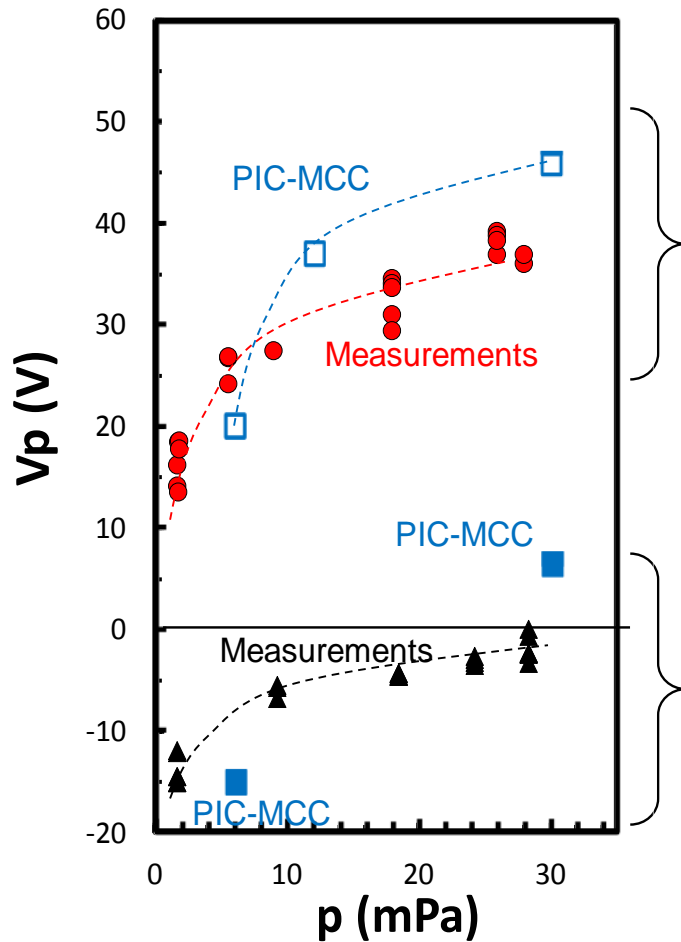
- ▲ electron mode, beam dump bias 0 V
- ▲ electron mode, beam dump bias 50 V

●, ▲ calorim. 50V
 Plasma potential from ion mode: $0 < V_p < V_{cal}$

●, ▲ calorim. 0V
 Plasma potential from electron mode: $V_p < V_{cal} = 0V$

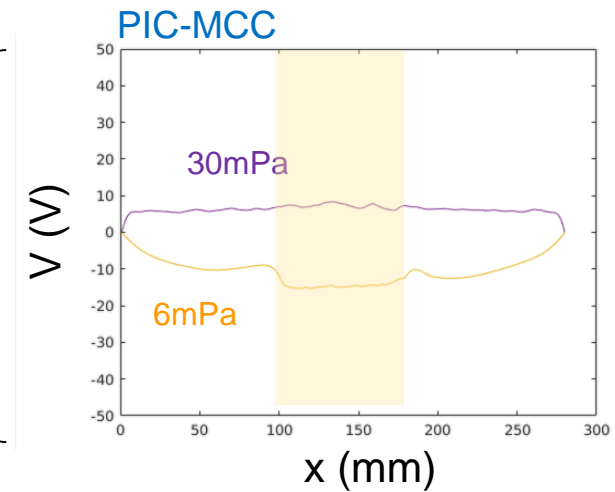
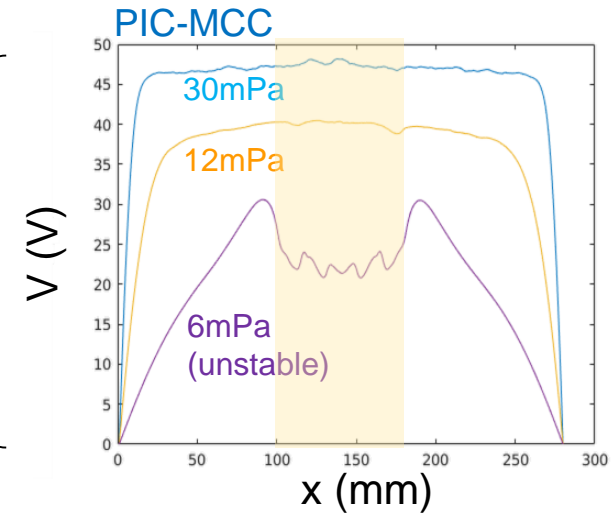


Measurements vs. PIC-MCC



$V_{cal} = 50V$

$V_{cal} = 0V$



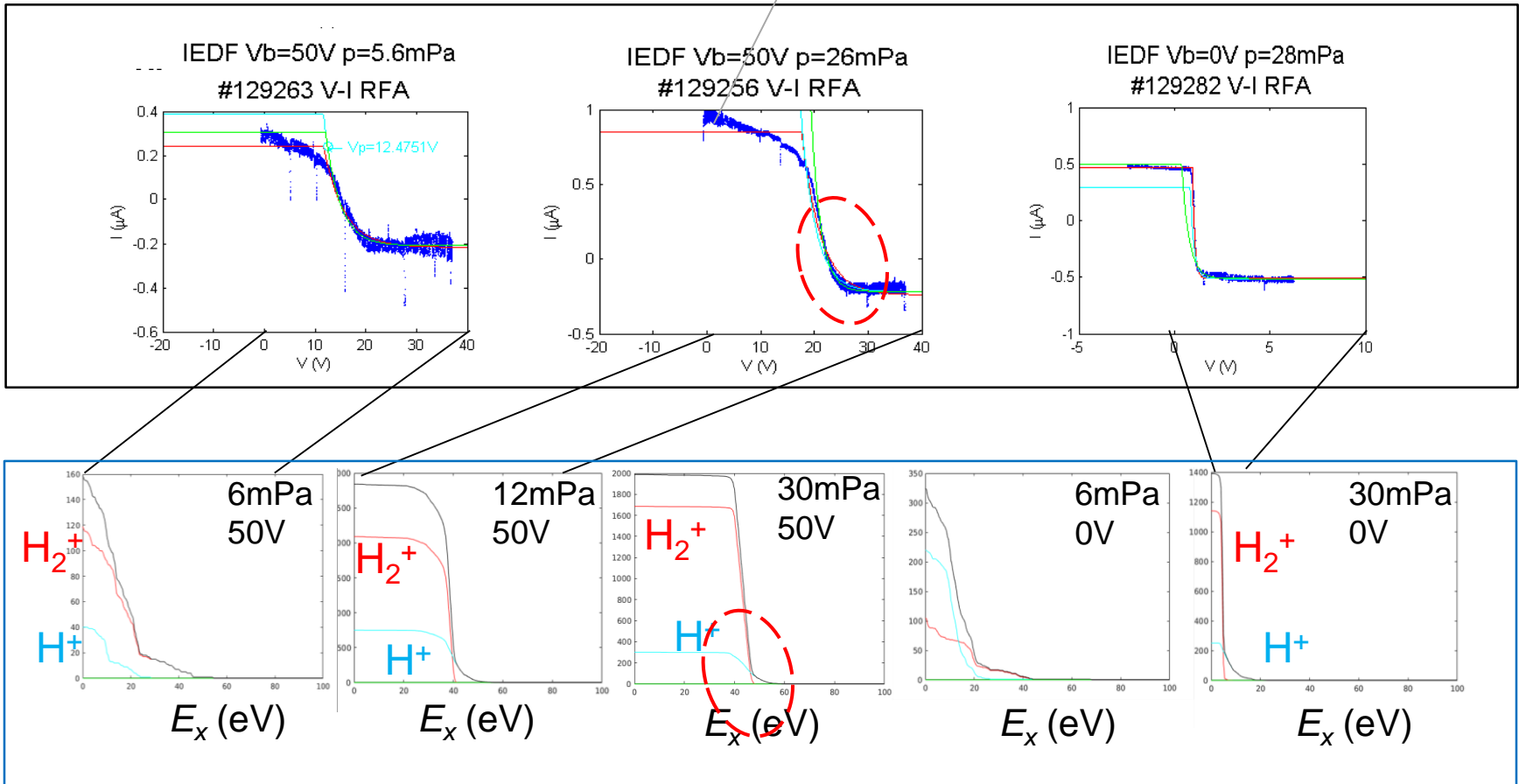
2) RFA CHARACTERISTICS: ION TEMPERATURE



Energy distribution of H_2^+ and protons is overlapped

Measurements: RFA characteristic

saturation affected by transfer function of RFA

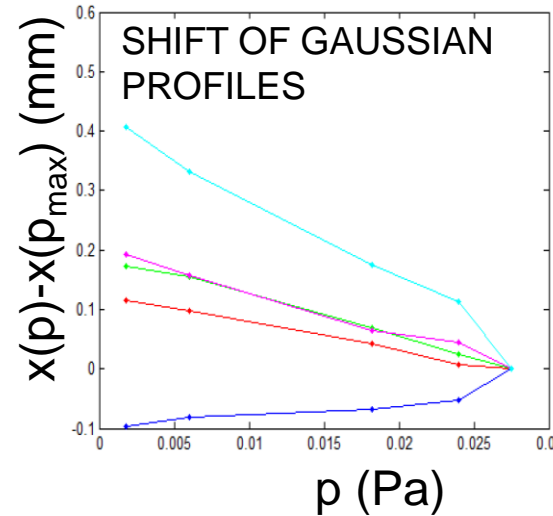
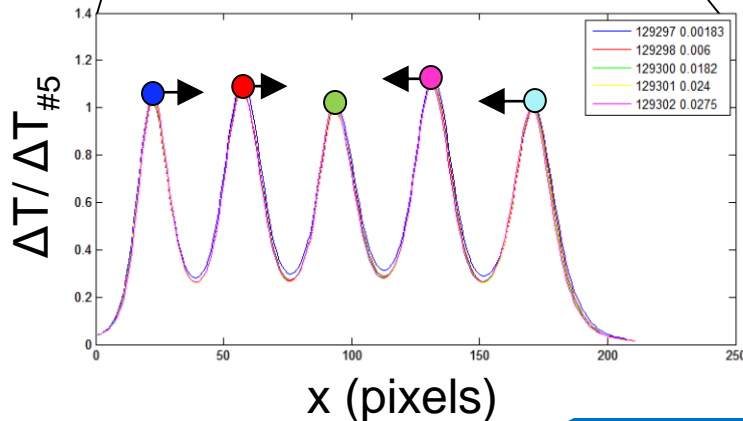
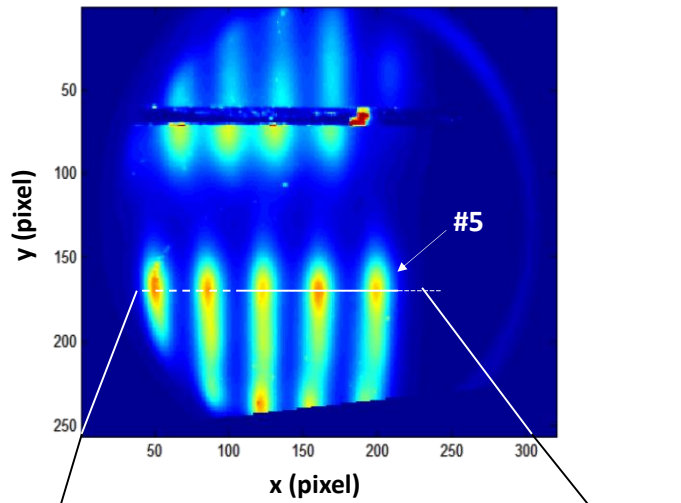


PIC-MCC: energy distribution of particles exiting from side walls

3) EFFECTS ON BEAM: MULTIBEAMLET OPTICS



Fitting ΔT profile produce **beamlet centre** : beamlet are getting closer one to the other



The centre of the edge beamlet footprint moves by about 0.5 mm/25mPa

FILTER BEAM PULSES:

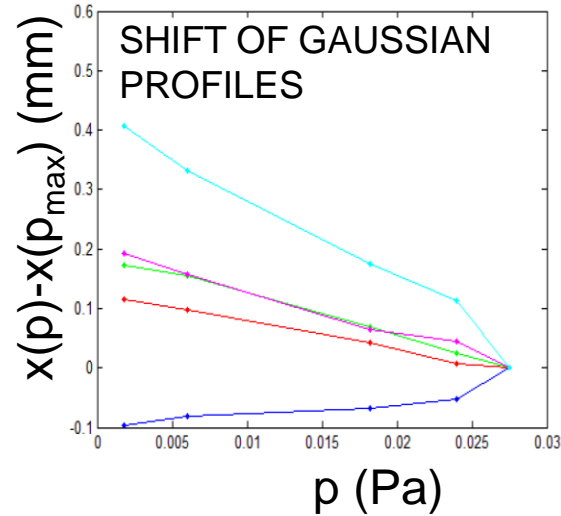
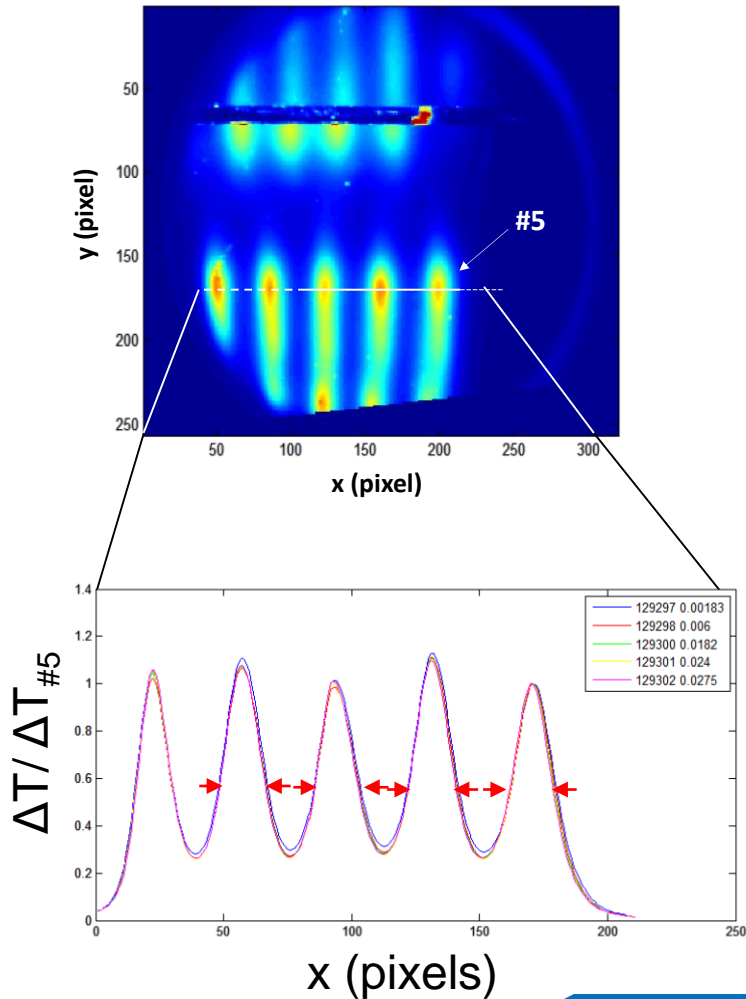
- arc power within +/- 5%,
- of +/- 3.5% with respect to the average ΔT was chosen
- initial temperature of the graphite tile was within +/- 4% with respect to the average one

3) EFFECTS ON BEAM: SINGLE BEAMLET OPTICS

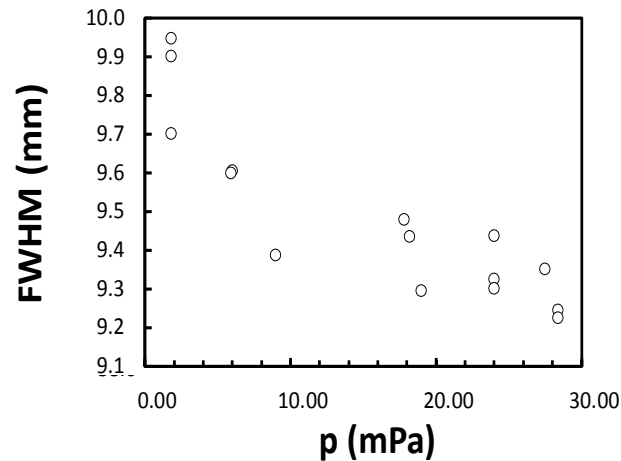


Fitting ΔT profile produce **beamlet centre** : beamlet are getting closer one to the other

Fitting ΔT profile produce **beamlet width**: focusing effect increasing pressure



The centre of the edge beamlet footprint moves by about 0.5 mm/25mPa



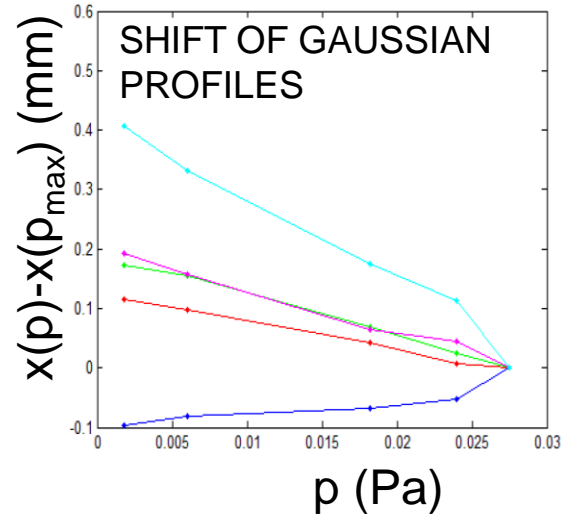
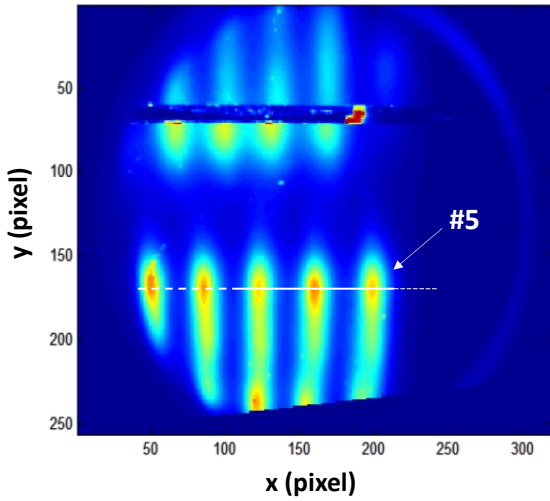
The beamlet FWHM is reduced by >5% in the pressure interval between 2mPa and 28mPa.

3) EFFECTS ON BEAM: SINGLE BEAMLET OPTICS



Fitting ΔT profile produce **beamlet centre** : beamlet are getting closer one to the other

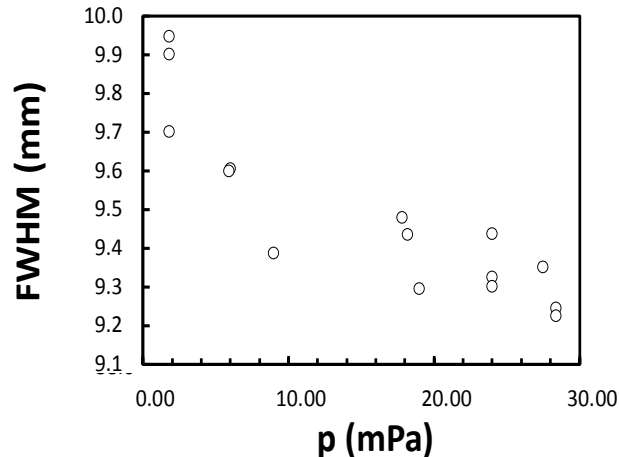
Fitting ΔT profile produce **beamlet width**: focusing effect increasing pressure



The centre of the edge beamlet footprint moves by about 0.5 mm/25mPa

Multi-beamlet \rightarrow decreasing repulsion
- transverse electric field 1 V/cm along 1m

Single-beamlet \rightarrow focusing
- vary compensation degree ψ by +0.7%



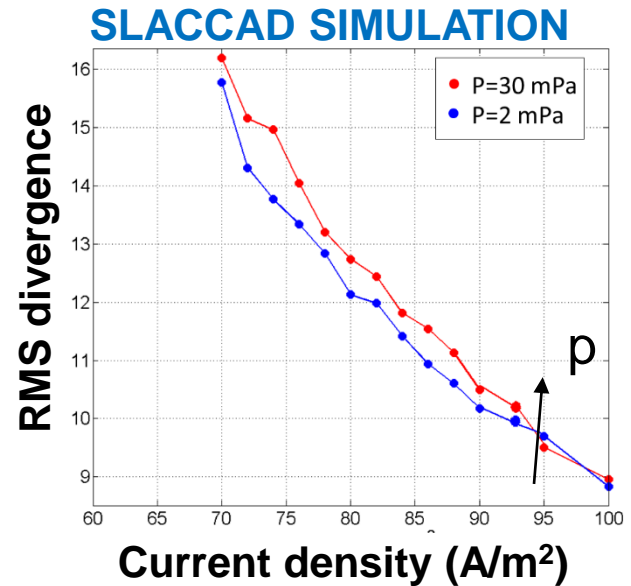
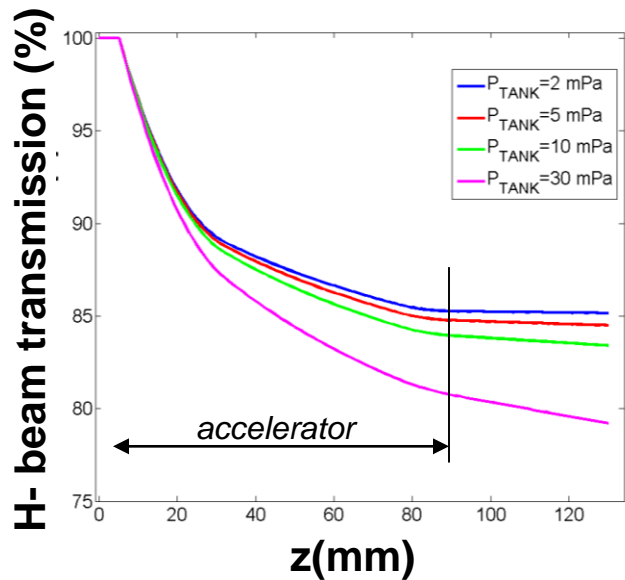
The beamlet FWHM is reduced by >5% in the pressure interval between 2mPa and 28mPa.

3) EFFECTS ON BEAM OPTICS

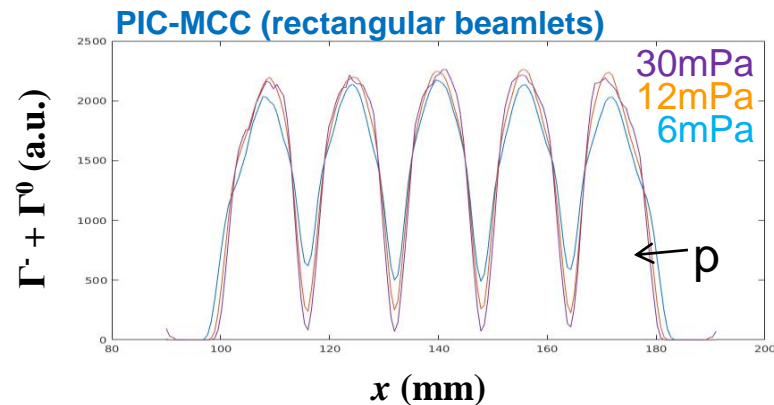
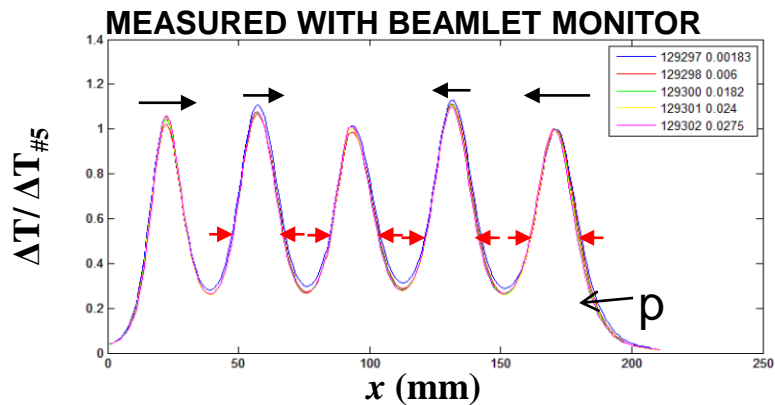
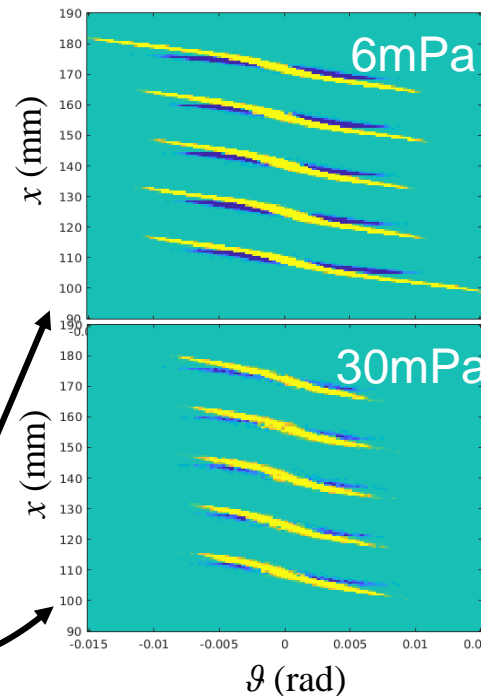
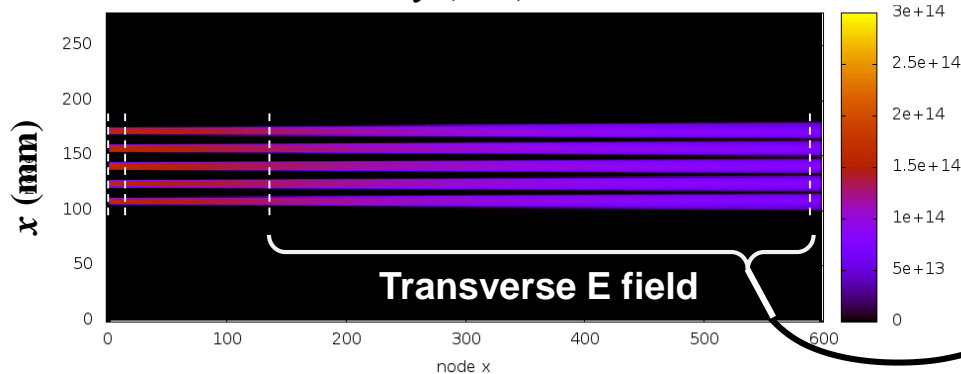
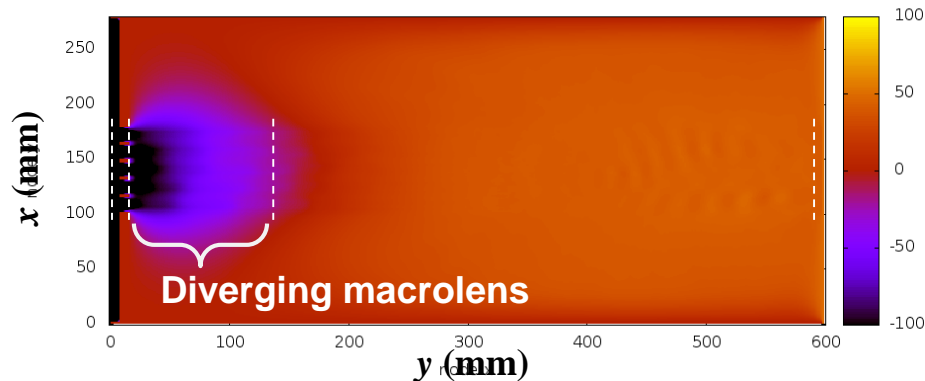


Very small effect but the trend is always present – hot to distinguish between space charge effects inside the accelerator or after?

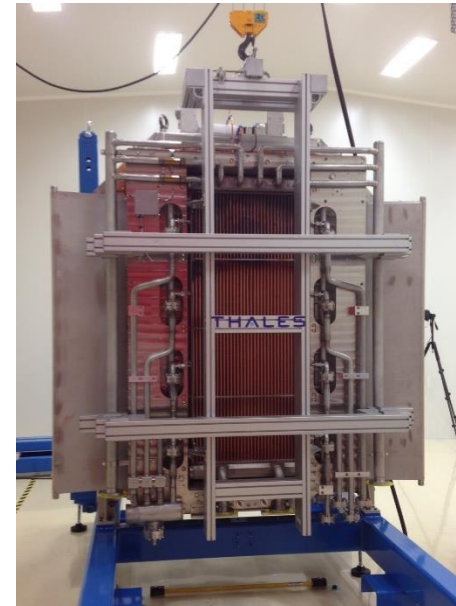
Ray-tracing iterative poisson solver SLACCAD simulations of the accelerator, including stripping: optics getting worse when increasing tank pressure



3) EFFECTS ON BEAM OPTICS: PIC-MCC



- **Beam plasma:** plasma potential set by beam dump bias (lower than calorimeter potential due to secondary emission electrons); cold H_2^+ and relatively hot H^+
- **Beam focusing when increasing tank pressure from 2 to 30mPa:** small multi-beamlet steering effect (0.5mm/m); small single-beamlet focusing by 0.5mrad (SLACCAD calculations gives increasing divergence when increasing stripping losses!)
- **PIC-MCC in agreement w/ measurements:** scaling to ITER HNB and the two prototypes SPIDER and MITICA



ITER BEAM SOURCE (SPIDER) – SEPT 2017



ITER NEUTRAL BEAM TEST FACILITY - PADOVA



Reaction	notes
$\underline{H}, H_2 \rightarrow \underline{H}^+, 2e, H_2$	Fast electron
$\underline{H}, H_2 \rightarrow \underline{H}, e, H_2$	fast electron
$\underline{H}, H_2 \rightarrow \underline{H}, H_2^+, e$	slow ion at RT, Rudd electrons
$\underline{H}, H_2 \rightarrow \underline{H}, H^+, e, H$	
$\underline{H}, H_2 \rightarrow \underline{H}, H^+, H^+, 2e$	
$\underline{H}, H_2 \rightarrow \underline{H}^+, e, H_2$	
$\underline{H}, H_2 \rightarrow \underline{H}, H_2^+, e$	slow ion at RT, Rudd electrons
$\underline{H}, H_2 \rightarrow \underline{H}, H_2^+$	slow ion at RT
$\underline{H}, H_2 \rightarrow \underline{H}, H^+, e, H$	slow ion at 7eV, peak at 90° and 270°
$\underline{H}, H_2 \rightarrow \underline{H}, H^+, e, H$	cold slow ions
$\underline{H}, H_2 \rightarrow \underline{H}, H^+, H^+, 2e$	slow ions at 9eV, isotropic
$\underline{H}^+, H_2 \rightarrow \underline{H}^+, H_2^+, e$	slow ion at RT, Rudd electrons
$\underline{H}^+, H_2 \rightarrow \underline{H}, H_2^+$	slow ion at RT
$\underline{H}^+, H_2 \rightarrow \underline{H}^+, H^+, e, H$	
$\underline{H}^+, H_2 \rightarrow \underline{H}^+, H^+, H^+, 2e$	slow ions at 10eV, isotropic
$\underline{H}^+, H_2 \rightarrow \underline{H}^+, H_2$ (elastic)	
$H_2^+, H_2 \rightarrow H^+, H, H_2$	
$H_2^+, H_2 \rightarrow H_3^+, H$	ion at RT (rotational exc.)
$H_2^+, H_2 \rightarrow H_2, H_2^+$	slow ion at RT
$H_2^+, H_2 \rightarrow H_2^+, H_2$ (elastic)	
$H_2^+, H_2 \rightarrow H_2^+, H_2$ (elastic)	
$H_3^+, H_2 \rightarrow H, H_2^+, H_2$	
$H_3^+, H_2 \rightarrow H_2, H^+, H_2$	
$H_3^+, H_2 \rightarrow H^+, H_2, H_2$	
$H_3^+, H_2 \rightarrow H_2^+, H, H_2$	
$H_3^+, H_2 \rightarrow H_3^+, H_2$ (elastic)	